Application of graphene-based flexible antennas in consumer electronic devices

ELSEVIER

Application of graphene-based flexible antennas in consumer electronic devices

A. Scidà [1], S. Haque [2,†], E. Treossi [1,*], A. Robinson [3,†], S. Smerzi [4], S. Ravesi [4], S. Borini [5,†], V. Palermo [1,6,*]

[1] Institute of Organic Synthesis and Photoreactivity (ISOF), National Research Council of Italy (CNR), Via P. Gobetti 101, I-40129 Bologna, Italy
[2] Emberion Limited UK, Sheraton House, Castle Park, Cambridge CB3 0AX, UK
[3] Beko R&D UK, 12 Science Park, Milton Road, Cambridge CB4 0F, UK
[4] STMicroelectronics, Stradale Primosole, 50 95121 Catania, Italy
[5] Graphitene Ltd, SBC Open Innovation Campus, Stevenage, Herts SG1 2FX, UK
[6] Chalmers University of Technology, Department of Industrial and Materials Science, Hörsalsvägen 7A, Goteborg, Sweden

We describe the fabrication and characterization of Near-Field Communication (NFC) devices based on highly flexible, carbon-based antennas composed of stacked graphene multilayers. This material features a high value of conductivity (4.20 * 10^5 S/m) comparable to monocrystalline graphite, but is much more flexible and processable. We first studied the replacement of metal with carbon antennas using computer modeling, to select the best design. Then we manufactured several devices to be used according to the communication protocol ISO/IEC 15693. The inductance of the G-paper antennas was tested before and after hundreds of thousands of bending cycles at bending radii of 45 and 90 mm. During bending the self-resonance frequency and inductance peak showed minimal variation and the resistance at 1 MHz changed from 33.09 Ω to 34.18 Ω, outperforming standard, commercial metallic antennas. The devices were successfully tested by exchanging data with a smartphone and other commercial NFC readers, matching the performance of standard, commercial metallic antennas. The graphene antennas could be deposited on different standard polymeric substrates or on textiles. Smart cards, flexible NFC tags and wearable NFC bracelets were prepared in this way to be used in electronic keys, business cards and other typical NFC applications.

Introduction

A key target for modern technology is to replace metals with lighter, cheaper, less energy-consuming materials. This "metal replacement" goal is already well established for structural applications in aeronautics and automotive, where the search for higher efficiency and reduced CO_2 emission is pushing toward the use of carbon-based materials (e.g. carbon fiber composites and high-performance polymers), replacing up to 50% of the metal parts of the vehicle [1].

Metal replacement in "functional" applications, such as in cables or electronics, is equally important due to the huge recent increase in electronic waste [2] and the necessity to reduce waste management problems associated with heavy metals [3], which are not destroyed by incineration and shall become air pollutants [4].

This task is however more challenging compared to structural applications, due to the difficulty to match the high conductivity of metals (>10^7 S/m). Copper, aluminum, or silver have high electrical conductivity and excellent mechanical properties when shaped into thin films; however, they have a high cost in terms

* Corresponding authors at: Institute of Organic Synthesis and Photoreactivity (ISOF), National Research Council of Italy (CNR), Via P. Gobetti 101, I-40129 Bologna, Italy.
E-mail addresses: Treossi, E. (treossi@isof.cnr.it), Palermo, V. (palermo@chalmers.se).
† Affiliation at the time when the work was done: Nokia Technologies, Broers Building, Cambridge CB3 0FA, UK.

https://doi.org/10.1016/j.mattod.2018.01.007

of thermal energy, high specific weight, and can possibly oxidize and be corroded. The production of disposable antennas typically involves patterning and chemical etching of such metals to create the conducting circuits of the antenna. Chemical etching is a process that comprises many steps and requires numerous pollutant chemical agents, which could also damage the underlying substrate, and thus narrow down the range of substrates suitable for antenna production. Thus, new technological solutions would be required to replace metal circuits with disposable and environmentally friendly materials.

An attractive way to produce conductive patterns on rigid or flexible substrates is by printing of conductive ink solutions; this approach features low manufacturing cost and can be suitable for industrial scale-up. While average conductivity can be obtained easily in this way, high temperature annealing of the printed inks is often required to reduce electrical resistivity. The annealing can degrade or deform the underlying polymeric substrate and limits applications on textiles. Metallic nanoparticles are also frequently used in conducting inks used for printing antennas. Such particles, due to their high surface area, can interact with atmospheric water or oxygen, causing the antenna to oxidize and degrade more rapidly than bulk metals. In many applications, as example in wearable electronics, antennas have to withstand harsh chemical environment and therefore they have to be corrosion-resistant (as example thanks to a suitable protective coating). One possible solution to this problem is to use carbon-based materials, resistant to corrosion, featuring high thermal, chemical, and mechanical stability.

Graphene is a monolayer of carbon atoms, arranged in a honeycomb lattice. A monolayer of this material could, ideally, outperform even the most conductive metal (silver or copper). The high mobility of charges in graphene ($\mu \approx 10^5\ cm^2\ V^{-1}s^{-1}$) combined with its high charge density ($n \approx 10^{13}\ cm^{-2}$) [5] yields a conductivity $\sigma = ne\mu \approx 4.9 \times 10^8\ S/m$, allowing to achieve sheet resistance of <30 Ω/□ combined with 90% optical transparency [6].

Graphene monolayers shall now be produced on large scale and replace transparent conductors, as example in flexible displays or in solar cells [7]. Practical applications requiring the transport of significant currents, such as NFC antennas or power electronics, require however sheet resistance $\ll 1\ \Omega/\square$.

In the last few years, the development of graphene exfoliation techniques has allowed the production of graphene-based materials (graphene solutions, graphene oxide etc.) on a large scale and at low cost. These graphene-based materials, featuring high anisotropic 2-dimensional shape and good processability, shall be re-assembled in thick, flexible layers forming "graphene paper" (G-paper) with properties different from normal, crystalline bulk graphite [8]. The good mechanical and electrical properties of these materials, together with their cheap and easy production methods, allow their use as conductive flexible electrodes in capacitors [9], gas permeation barriers [10], or even light-emitting electrical conductor in incandescent bulbs [11]. This approach of exfoliation and reassembling has been successfully used also for other 2D materials; noteworthy, it can be used to produce new composite materials, featuring a disordered staking of different 2D nanosheets or even a combination of 2D and 1D nanostructures [12].

TABLE 1

Electrical conductivity of materials composed of 2-dimensional nanosheets, collected from published research papers.

Device tested	Conductivity (S/m)	References
–	$\approx 10^6$	Monocrystalline Graphite [18]
Multiple coiled antenna for NFC communication	$4.20 \cdot 10^5$	This work
Dipole antenna for RFID	$5.10 \cdot 10^4$	[17]
Dipole antenna	$4.30 \cdot 10^4$	[14]
Transmission lines, wideband antenna	$4.30 \cdot 10^4$	[13,15]
Dipole antenna	$2.45 \cdot 10^4$	[16]
UHF RFID tag	$1.39 \cdot 10^4$	[43]
Conductive patterns	$1.00 \cdot 10^4$	[44]
Conductive patterns (MoS_2)	$3.00 \cdot 10^3$	[45]
Conductive patterns	870	[46]
Emitting filament in light bulb	16	[11]

The use of "graphene paper" as a good conductor for antennas has already been demonstrated in recent works [13–17] mostly for dipole antennas; such antennas have though less stringent requirements than standard mass-scale consumer electronic devices based on NFC protocols. In these recent works, carbon-based materials with a conductivity from 10^2 S/m to 10^4 S/m were used, at least two orders of magnitude lower than the one of ideal graphite ($\approx 10^6$ S/m) [18]. Table 1 gives a representative list of works published on graphene-based antennas or highly conductive patterns.

While the nice performance of G-paper for electronics has been demonstrated at a lab scale, there is still no concrete example of graphene outperforming standard metals in commercial electronic applications, a major challenge for the industrial development of graphene technology.

In this work, we thus describe a graphene-based paper featuring a high value of conductivity ($4.20 * 10^5$ S/m) comparable to monocrystalline graphite, but much more flexible and processable. Starting from these good properties, we demonstrate the technological maturity of this material by producing, characterizing, and modeling antennas based on it, demonstrating that they could be successfully employed in short-range, near-field applications (NFC) in replacement of current metallic commercial antennas, outperforming any other carbon-based conductor. We obtained high performance, thanks to intense optimization of the devices: first, we performed a systematic comparison and selection of different starting materials, either produced in lab or available commercially at low cost and large scale. This extensive benchmarking of materials' properties was then used as input for computational modeling, to select the optimal design of the antenna. Then, the selected designs were produced by blade cutting or laser machining, followed by lamination of the antennas on various rigid or flexible substrates (plastic or cardboard) and even textiles (silk). Finally, the performance of the device was evaluated including it in Near Field Communica-

tion (NFC) tags able to exchange data with commercial NFC readers and with standard mobile phones.

These antennas are composed of pure carbon-containing nanoplatelets, without any additional binder or metallic additive, do not require high-temperature annealing and could withstand hundreds of thousands of bending cycles without performance degradation.

The selection of materials, device geometry, and processing techniques allowed the antennas to be 100% compatible with standard technology and to be used directly to replace metal-based antennas in radio-frequency identification (RFID) devices.

Materials and methods

Home-made graphene paper was realized with graphene nanoplatelets provided by Avanzare, Spain (AVA18, D50 = 50 μm) by compression of the powder at 200 Bar at room temperature, achieved with a Hydraulic Compact Press (Figure 1a). We also used graphene papers provided by two different commercial producers: XG-Science, USA (product: XG-Leaf B) and NANESA, Italy (product: G2nan-sheet GS50).

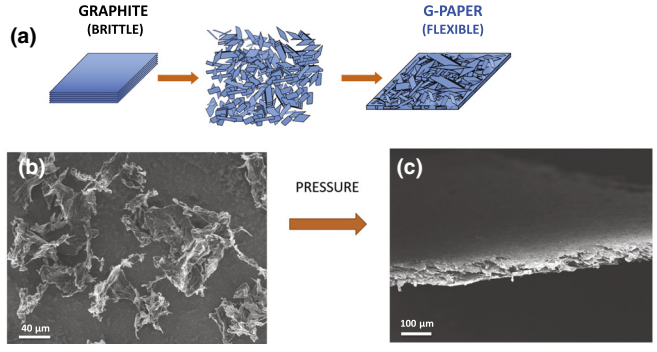

FIGURE 1

(a) Scheme describing the process used to produce graphene paper from exfoliated graphene nanoplatelets. (b and c) SEM images of (b) the graphene nanoplatelets used in the experiments and (c) the graphene paper realized.

CAD modeling tools (CATIA, ST RFID.exe software) were used to predict the electrical resistance, inductance, and capacitance of several antenna designs, and select the most suitable one.

The antennas were deposited on different substrates: polyethylene terephthalate (PET), Kapton, polyethylene naphthalate (PEN), polycarbonate (PC), polyvinyl chloride (PVC), paper and silk. The antennas were bonded to different commercial NFC integrated circuits (STMicroelectronics M24LR04E-R [19,20], NXP ICODE SL2S2002 [21] or NXP Mifare UL MF0ICU1 [22]).

Graphene paper was patterned using two different approaches: a robotic cutting plotter from Silhouette Cameo and a laser system Trotec speedy 300, which were used for precision cutting of the graphene paper (Figure 2).

Structural characterization of the samples was performed using a Scanning Electron Microscope (SEM) LEO 1530 FEG, equipped with an Energy Dispersive X-ray Spectrometer (EDS) Oxford, Silicon Drift Detector (SDD), INCA software, for elemental analysis. XRD measurements were collected with a PANalytical X'PertPro instrument in Bragg–Brentano reflection mode.

Measurements of electrical conductivity were performed using a 4-probe setup, using an Agilent E3612A as current generator and a Keithley 6514 as voltmeter.

The impedance of the NFC antennas was measured with respect to frequency variation by an impedance analyzer HP 4294A.

The bending test on graphene paper antennas was performed using a custom made bending system (Bose). The sample was placed on the 4-point bending system and calibrated so that a minimum bending radius of 45 mm could be achieved.

The performance of the graphene-based antennas was tested with a STMicroelectronics CR95HF RF Transceiver, a commercial smartphone (Samsung S3), and an electronic lock (Iseo Serrature s.p.a., Italy).

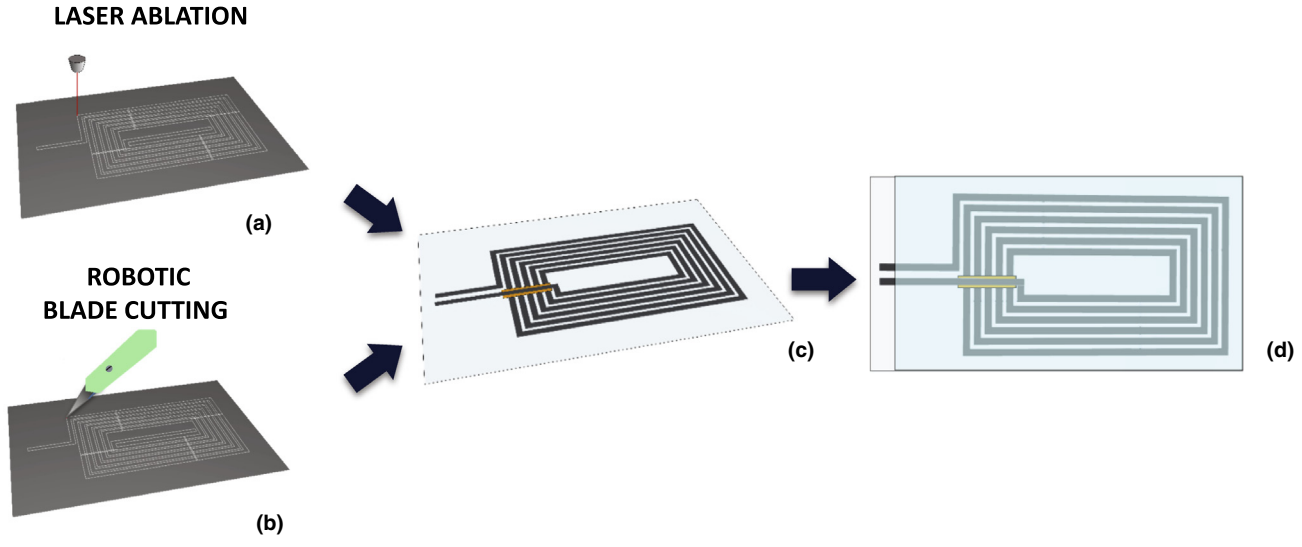

FIGURE 2

Fabrication process of the graphene antenna: (a) laser ablation or (b) blade cutting, (c) lamination of the first substrate with feed line folded on an insulating stripe, (d) lamination of the final antenna.

Results

We first compared the electrical conductivity of different types of G-paper (either commercially available or produced in the lab) to select and use the highest performing material as carbon-based conductor. Highly ordered G-paper is usually obtained by filtration of a graphene oxide solution [10] (followed by a reduction step), or by deposition of graphene, graphene nanoplatelets, or reduced graphene oxide on a substrate. In some of these methods, dispersants and/or high boiling solvents are involved in the processes, which remain in the final material even after washing, thus lowering electrical resistance. Annealing at high temperature is often needed to improve the conductivity of graphene membranes and films of several orders of magnitude [13–15,23–25]. Instead of solvent processing, we decided to use a solvent-free method using graphene nanoplatelets as starting material, which once compressed yielded a mechanically robust and bendable layer, with most of the single platelets aligned along the plane.

We thus prepared several samples of home-made graphene paper starting from nanoplatelets commercially available (producer: Avanzare, Spain [26]), featuring an average lateral size (D50) of 50 μm. The G-paper was created by compression of the powder at 200 Bar at room temperature with a Hydraulic Compact Press (Figures 1 and S1). Unlike what is needed for other applications of graphene, this procedure does not require to use monolayers, but shall be performed using cheaper, multilayer platelets, commercially available on kilograms scale. The pressure aligned the nanoplatelets and compacted them into a continuous, robust material, decreasing thus the high resistivity, which is always present between neighboring flakes in graphene-based conductive layers deposited from solution [27]. Commercial G-paper, obtained from XG-Science, USA (XG-Leaf B) and NANESA, Italy (G2nan-sheet GS50) was also tested and used for the realization of the antennas.

We performed structural and electrical characterization on each G-paper tested. The material was composed by crystalline domains, stacked on top of each other along *z*-axis, i.e. perpendicular to the G-paper plane; each domain was formed by 100–200 monolayers of graphene as estimated by XRD using Scherrer's law and the full width at half maximum (FWHM) of the 002 peak typical of graphite. The chemical composition of each sample was estimated by EDX; as expected, all G-paper samples were composed mostly by carbon (>97% wt) with traces of oxygen (≈2% wt) and very low amounts of other elements. This excluded (especially for commercial products) the presence of metallic conductive additives such as Au, Ag, or Cu. It excluded as well the presence of solvents containing nitrogen or chlorine, as example dimethylformamide, N-methyl-2-pyrrolidone, or dichlorobenzene (typically used for graphene production in liquids), which could decrease the electric conductivity.

Then, four-probe measurements were performed to obtain the sheet resistance R_s using an Agilent E3612A as current generator and a Keithley 6514 as voltmeter. The electrical conductivity $\sigma = R_s/t$ for each material was calculated using the measured R_s and the thickness t. All samples, both commercial and fabricated in house, showed very good electrical conductivity ($\sigma > 10^4$ S/m), as reported in Table 2.

TABLE 2

Measured sheet resistance and related bulk conductivity of the materials tested.

Material	Measured thickness (μm)	Measured sheet resistance (Ω/sq)	Measured conductivity (S/m)
XG-Leaf B	55 ± 5	0.043 ± 0.007	$(4.2 \pm 0.8) \cdot 10^5$
Nanesa GS-50	66 ± 9	0.11 ± 0.03	$(1.4 \pm 0.4) \cdot 10^5$
CNR	62 ± 8	0.19 ± 0.03	$(8.5 \pm 1.7) \cdot 10^4$

The conductivity of the materials was also measured upon mechanical bending. Patterned, linear stripes of G-paper featured a constant electrical resistance during time and under mechanical stress, showing no change upon extensive cycles of bending. Figure S2 in Supporting Information shows the changes in electrical resistance observed during fatigue bending cycles, normalized to the initial value of the sample, confirming the high reproducibility and stability of the measured electrical performance. No significant difference was observed using polymeric substrates of different thicknesses (50–125 μm), leaving the material uncoated or, conversely, embedding it between two polymeric layers.

Noteworthy, samples produced industrially showed higher conductivity than samples prepared in lab, either prepared for this work (Table 2) or reported in literature (Table 1). The electrical parameters of the material with the lowest sheet resistance (XG leaf-B) were thus used as input to design the target antenna.

After measuring the conductivity of simple linear patterns, we modeled by simulations several antenna designs, in order to achieve the highest performance. We modeled the antenna for application in one of the most widely used communication protocol RFID standard, the ISO/IEC 15693 [26]. The antenna has the role to enable the communication between the active reader (e.g., a smartphone) and the passive tag through the radio-interface operating in the RF ISM band of 13.56 MHz. In NFC systems, reader and tag are magnetically coupled by their inductive loop antennas. A battery is not required to access the tag, whether in write or read mode, since the tag harvests the energy needed to operate from the magnetic field generated by the reader. The interrogation field strength is the minimum field strength H_{min} at which the voltage V_{ant} induced on terminals of the tag antenna is high enough to power and operate the tag [28]. Therefore, geometrical parameters for the tag antenna to be designed (i.e., area A, number of coils N, width W and spacing S of the conductive tracks) should be chosen to minimize the interrogation field strength H_{min}, which varies with the frequency: it reaches its minimum value when the tag antenna resonates with the transmission frequency of the reader [28]:

$$H_{min} = \frac{1}{\mu_o \cdot A \cdot N \cdot V_{ant}} \cdot \sqrt{\left(2P_{load}L + \frac{V_{ant}^2}{2\pi f_{res} Q}\right)^2 + \left(\frac{2P_{load}L}{Q}\right)^2} \quad (1)$$

In (1), P_{load} is the required minimum AC power (at the antenna terminals level) for the tag to properly work, L and Q are the equivalent inductance and quality factor $Q(f) = 2\pi f_{res}\, L/R_1$, R_1 is the equivalent series resistance of the tag antenna at the resonance frequency f_{res}. For a given antenna area A, the

number of turns N directly impacts the quality factor Q, which is the actual Figure of Merit (FOM) for the tag antenna design, since H_{min} is minimized when Q is at its highest value.

In Table 3 we report L, R_s and Q factor calculated for 27 different antenna designs using CAD software tools (CATIA, ST RFID. exe) [29,30]. The parameters used to define the conductive material in the modeling were the ones measured experimentally for the G-paper XG-leaf B, as described above; the total lateral size was fixed at 45 × 75 mm^2 (≈the standard size of a credit/debit card). Simulation results were parametrized respect to the geometrical parameters N, W, and S. The design giving the best quality factor had $N = 6$ coils and track width $W = 2$ mm. The spacing between adjacent coils was $S = 0.5$ mm, to increase the inductance, further enhancing the quality factor of the antenna.

To verify that the tag antenna design selected was suitable for a real NFC device we used (1) to plot the theoretical interrogation field strength H_{min} vs. the antenna quality factor Q in Figure 3; P_{load} and V_{ant} parameters were measured from a real commercial RFID harvester [19]. Any commercial reader, compliant to the ISO standard [31], must generate a magnetic field strength in a specified range of values H_{spec} between 0.15 and 5 A/m. The required quality factor Q_{req} for the tag antenna was thus defined using Figure 3. Comparison of the simulated performance of different antennas, summarized in Table 3, showed that the antenna with geometry $N = 6$ coils, width $W = 2$ mm and coil spacing $S = 0.5$ mm could give a required range $Q_{req} = 5.02$, allowing communication with any NFC-compliant commercial reader.

TABLE 3

Simulation results for graphene-based antennas (fixed parameters: area = 45 × 75 mm^2, thickness = 55 μm, material: XG-Leaf B).

N° of coils	Width (mm)	Spacing (mm)	L (μHr)	R_s (Ω)	Q (@13.56 MHz)
4	0.5	0.5	2.44	126	1.65
	0.5	1	2.12	123	1.47
	0.5	2	1.70	116	1.25
	1	0.5	1.99	61	2.78
	1	1	1.76	59	2.54
	1	2	1.42	56	2.16
	2	0.5	1.44	28	4.38
	2	1	1.28	27	4.04
	2	2	1.04	26	3.41
5	0.5	0.5	3.43	155	1.89
	0.5	1	2.90	150	1.65
	0.5	2	2.19	138	1.35
	1	0.5	2.74	74	3.15
	1	1	2.34	71	2.81
	1	2	1.78	65	2.33
	2	0.5	1.86	34	4.66
	2	1	1.60	32	4.26
	2	2	1.21	29	3.55
6	0.5	0.5	4.50	183	2.10
	0.5	1	3.69	178	1.77
	0.5	2	2.64	158	1.42
	1	0.5	3.49	86	3.46
	1	1	2.90	82	3.01
	1	2	2.10	73	2.45
	2	0.5	2.24	38	5.02
	2	1	1.85	36	4.38
	2	2	1.32	32	3.51

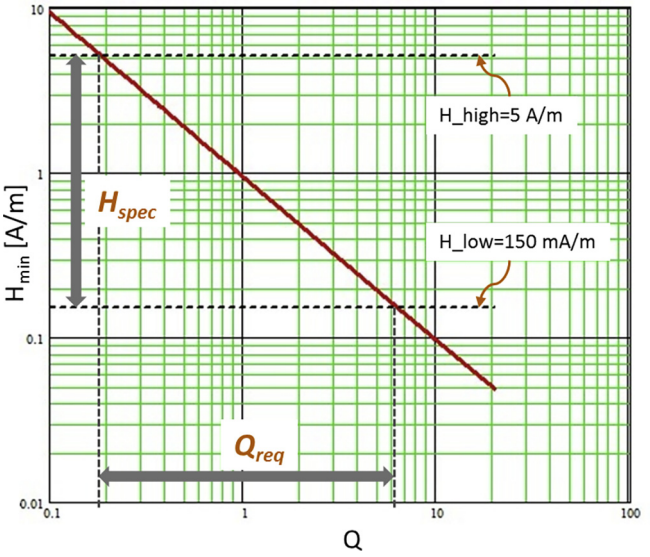

FIGURE 3

Simulated Log–Log plot of Interrogation Field Strength of a standard NFC reader (H_{min}) vs. Q factor (Q). Parameters: P_{load} = 20 μW, V_{ant} = 4Vpk-pk, A = 45 × 75 mm^2, $N = 6$, $W = 2$ mm, $S = 0.5$ mm (material used for the simulation: XG-LEAF B).

We did not limit experimental measurement only to the design giving bet performance, but produced six antenna prototypes with different geometrical design, with the total lateral size kept fixed to 45 × 75 mm^2 and the coils number fixed to 6. Two track widths, $W = 1$ mm and $W = 2$ mm were tested and, for each track width, three spacing, $S = 0.5$ mm, $S = 1$ mm and $S = 2$ mm, were implemented.

The antennas were eventually produced by patterning a continuous pre-fabricated G-paper with two different methods, laser ablation and mechanical cutting (Figure 2). These two different techniques are both compatible with industrial production, and showed no difference in the performance of the final device.

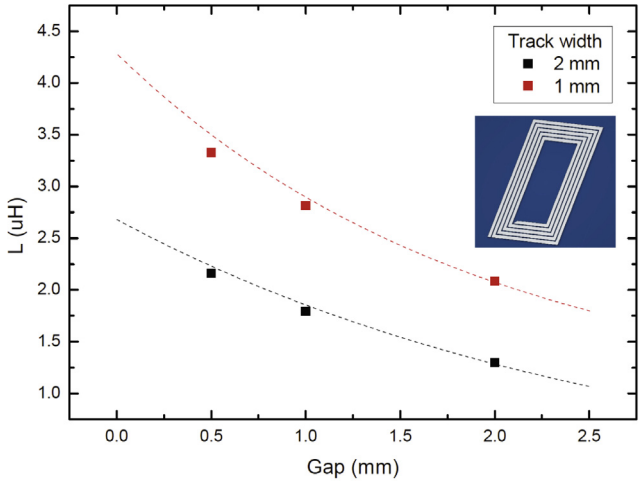

FIGURE 4

Inductance plots of antennas with different widths of the conductive track and spacing between coils, simulated using ST RFID software (dashed lines) and experimentally measured for 6 prototypes (square dots). The inset shows the computer rendering of one of the modeled devices.

Figure 4 compares the simulated plots of antenna equivalent inductance (dashed lines) with the experimental values measured at 1 MHz for the six implemented prototypes (square dots) patterned with the chosen geometry. The predicted and the measured results are within few% of the simulated results, confirming that the electrical properties of G-paper could be predicted using CAD modeling tools already used in conventional, metal-based electronics.

The equivalent inductance measured for the antennas is shown in Figure 5. The mechanical performance of the G-paper antennas was assessed by means of extensive bending tests using antennas deposited on PEN.

Figure 6a plots the inductance of the different G-paper antennas during one million bending cycles at bending radii of 45 and 90 mm (continuous lines). The inductance of a commercial metallic antenna (dashed line) [20] was also measured for comparison. Both the inductance (Figure 6a) and electrical resistance (Figure 6b) of the commercial antenna showed significant changes in position and intensity upon bending, much larger than the ones of the G-paper antenna. The self-resonance of the G-paper antenna showed remarkable stability after bending cycles. Self-resonance frequency changed slightly from 60.78 MHz to 60.79 MHz; inductance peak remained fixed at 52.41 MHz; inductance at 1 MHz showed a minimal variation (from 1.73 μH to 1.77 μH) while resistance at 1 MHz changed from 33.09 Ω to 34.18 Ω. Overall, the antenna showed a very good stability upon bending, better than the one of commercial, metal-based antennas (dashed lines in Figure 6).

The good performance and stability of the antenna allowed it to be useddirectly in standard electronic devices, without any additional optimization needed. To this aim, we first replaced the metallic antenna of a commercial NFC device from STMicroelectronics [20] (Flex M24LR04E, see Figures 7a,b and S3) using a standard electronic circuit for data storage. The metal antenna was removed and replaced with the selected G-paper antenna (i.e., $N = 6$, $W = 2$ mm, $S = 0.5$ mm). Thanks to the modeling

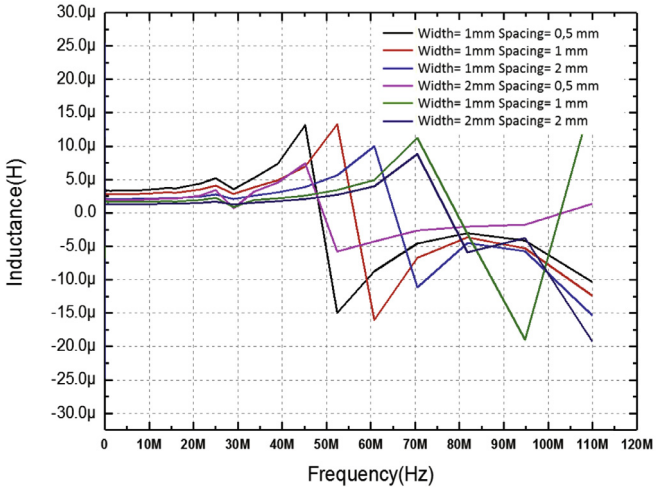

FIGURE 5

Equivalent inductance vs. frequency measured for six NFC coils of graphene paper with different geometrical parameters using a HP 4294A Impedance Analyser.

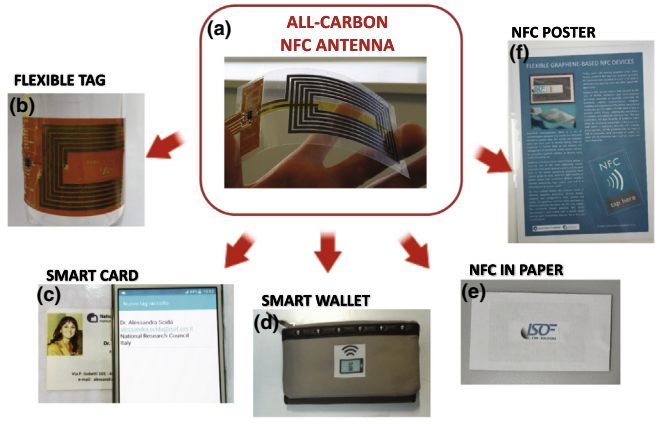

FIGURE 7

Examples of different applications of the carbon-based NFC devices.

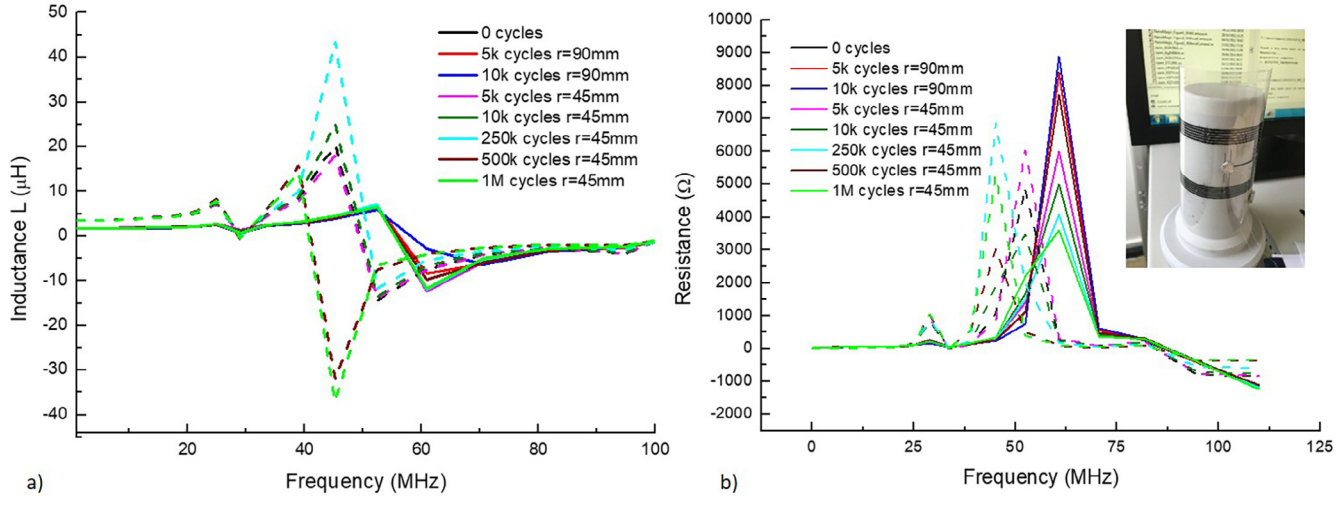

FIGURE 6

(a) Equivalent inductance and (b) electrical resistance of a commercial metallic antenna (dashed lines) and of graphene paper antenna (solid lines) vs frequency upon bending up to 1 million cycles at different bending radii *r*. Inset: picture of the bending test set-up.

and optimization work previously described, no change or tuning of the electronics was needed to go from metal-based to carbon-based conductor. By such arrangement, we checked experimentally that the G-paper antenna could be used to read or write information into the device with the conventional NFC protocol at 13.56 MHz. In particular, it was possible to wirelessly store and exchange data with the tag chip using an NFC app and a conventional smartphone (S3 model, Samsung, S. Korea) or a STMicroelectronics CR95HF RF Transceiver at a typical reading range of few centimeters. Due to the excellent stability, the device worked even when wrapped around curved objects (see Video V1 in Supporting information).

Besides using the G-paper antennas to replace metallic ones in existing devices (Figure 7a,b), we also realized new types of NFC tags on different substrates. A compact design could be achieved by bonding the antenna and a small NFC chip directly on paper (Figure 7e) or polymeric substrates (Figure 7f). In this way, we could produce smart cards to store and transmit data communicating with a smartphone (Figure 7c and Video V1), or to be used as an electronic key embedded in textiles to open standard electronic door locks (Figure 8 and Video V2). To test the long-term stability of the G-paper for such applications, we are currently using such G-paper devices as smart personnel keys to open the door of our lab, with no failure observed after more than one year of use.

The graphene-based antenna could be cut into different shapes and connected to several commercial integrated circuits, depending on the target applications. Thanks to the good stability and processability of the material, the antennas could be transferred onto a wide range of rigid or flexible substrates. We produced in this way NFC antennas embedded in different substrates like paper, PET, Kapton, PEN, PC, and PVC, see Figure S4. We did not observe any degradation of the graphene pattern after lamination and extensive bending on all substrates (see as example Figure 8a).

No changes in the antenna performance were observed upon direct prolonged exposure to the atmosphere or, conversely, upon application of an additional protecting coating.

Wearable devices and smart clothing are outstanding examples of flexible electronic applications, where the integration of electronic and telecommunication devices into textiles is highly desirable. To this aim, we realized a fully functional, flexible NFC tag with a graphene antenna embedded between two silk tapes integrated with an IC (Figure 8a,b). These devices could be used as a wearable bracelet (Figure 8c and Video V2) and also embedded in non-rigid clothing accessories (Figure 7d).

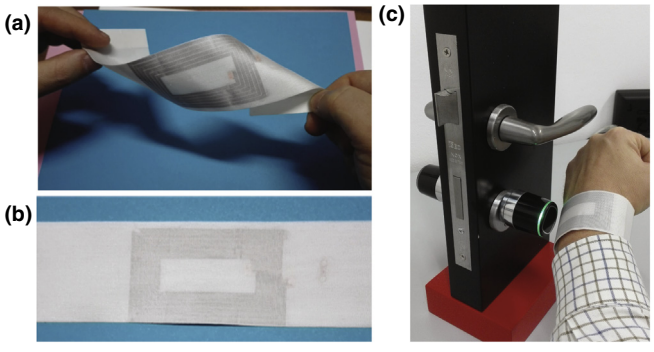

FIGURE 8

(a and b) Flexible, wearable NFC bracelet deposited on silk, (c) the NFC bracelet used to open an electronic lock.

Discussion and conclusions

The results described in this work demonstrate that it is possible to use G-paper to build fully working NFC antennas suitable for consumer electronics. It also confirms that highly flexible, all-carbon antennas shall have high stability upon bending fatigue.

The key step to ensure compatibility with industrial standard was the selection of high-performance G-paper and the careful modeling of the device geometry based on the material specifications. After the optimized design was achieved, the G-paper antennas could be used directly in working devices with no additional tuning of hardware or software needed for the pairing devices.

We discuss here briefly several key advantages of the use of all-carbon antennas for specific applications:

1) Resistance to bending fatigue. The intrinsic 2D layered nature of G-paper is ideal to withstand repeated bending cycles; it is well-known that, in graphite, graphene layers can easily slide over each other while maintaining a large adhesion energy, due to their π–π interactions; this is why exfoliation of graphite into graphene requires high shear forces and large energy input [32,33]. This same mechanism takes place in G-paper antennas, where upon bending the sheets can easily slide over each other to reduce applied stress, without however losing electrical percolation continuity due to the strong intra-sheet adhesion. This combination of facile sliding along the plane and difficult delamination across the plane is unique to 2D nanosheets in G-paper and not present in other nano-materials such as 1D nanowires or 3-dimensional, polycrystalline metallic layers. This causes the impressive mechanical and electrical stability observed after bending cycles, much different from the one of conventional, bulk graphite. Figure 6 shows that graphene paper antenna coils can withstand hundreds of thousands of cycles at various bending radii, with no changes of the resonance frequency or inductance at the working frequency, compared to a significant degradation or shift in the self-resonance frequency of commercial silver-based antennas.

2) Production costs. The devices presented in this work are basically G-paper-polymer stacks, composed by >97% in weight of carbon atoms. These devices cannot be defined as all-carbon electronics, because they still need a small silicon-based microchip to store information. However, the amount of metal present in these products is much lower than what is present in conventional ones; this could be a major advantage to reduce the cost of the final disposal of these cards, especially for applications where millions and millions of these devices are produced and trashed away after short time (e.g. conference badges, hotel room or swimming pool cards, smart advertising, internet-of-things products etc.).

It is impossible to perform a precise life-cycle analysis (LCA) of these materials, because the outcome would depend strongly on the production method and final application. However, the use of carbon-based materials in metal replacement for structural applications can give >50% reduction in processing time and

>20% reduction of CO_2 emissions [34]. These saving could be even more relevant for large-scale applications, e.g. disposable RFID (business cards, conference tickets, advertising etc.) where production time and final cost are very important.

3) Disposal issues. Beside production, also disposal could, in principle, be advantageous for these carbon-based antennas, because they do not contain heavy metals, a critical polluting agent in the disposal of electronic devices [35] widely present in natural waters [36]. The possible toxicity of graphene-based materials for humans and in the environment is intensively studied in these years, and first results show that pure 2D material shall have low toxicity [37,38] and good bio-degradation in water [39]. We expect even lower potential danger for G-paper as compared to highly exfoliated nanosheets, due to the dense, compact shape of the material. While heavy metals are easily oxidized and converted in water-soluble ions, G-paper, similarly to graphite, is chemically inert and insoluble in water. Finally, carbon-based conductors are also interesting for wearable biomedical and sensing applications, thanks to their tunable interaction with other carbon-based materials such as paper, polymer substrates (as the ones used here) as well as biological cells and molecules [40–42].

While tens of potential applications of graphene have been demonstrated at the prototype level [7], the successful development of graphene-based technology will take place only if we will be able to move from lab-scale, material-centered prototypes to fully functional demonstrators, directly compatible with existing technological protocols, and able to interact with devices already commercial. The antennas described in this work could, in principle, represent a first step toward competitive applications of carbon-based materials in the field of analogic and telecommunication electronics.

Acknowledgements

The research leading to these results has received funding from the European Union's Horizon 2020 research and innovation program under grant agreement n°696656 – Graphene Flagship and grant agreement n°642196 – Marie-Curie ITN-iSwitch. We thank M. Gazzano, Franco Corticelli and Alessio Nubile, for the support and the expertise given in the research.

Appendix A. Supplementary data

Supplementary data associated with this article can be found, in the online version, at https://doi.org/10.1016/j.mattod.2018.01.007.

References

[1] Airbus. http://www.airbus.com/newsevents/news-events-single/detail/composites-help-keep-next-generation-airbus-aircraft-eco-efficient/.
[2] Press-release. http://europa.eu/rapid/press-release_IP-15-6203_en.htm.
[3] EUR-Lex. http://eur-lex.europa.eu/legal-content/EN/TXT/?uri=CELEX:32011L0065.
[4] C.C. Lee, G.L. Huffman, ACS Symp. Ser. 515 (1993) 189–198.
[5] A.K. Geim, K.S. Novoselov, Nat. Mater. 6 (2007) 183–191.
[6] S. Bae et al., Nat. Nanotechnol. 5 (2010) 574–578.
[7] A.C. Ferrari et al., Nanoscale 7 (2015) 4598–4810, https://doi.org/10.1039/c4nr01600a.
[8] D.A. Dikin et al., Nature 448 (2007) 457–460.
[9] Z.Y. Xia et al., ChemPlusChem 79 (2014) 439–446, https://doi.org/10.1002/cplu.201300375.
[10] D. Pierleoni et al., Carbon 96 (2016) 503–512. doi: 10.1016/j.carbon.2015.09.090.
[11] F.J. Tolle, M. Fabritius, R. Mulhaupt, Adv. Funct. Mater. 22 (2012) 1136–1144, https://doi.org/10.1002/adfm.201102888.
[12] J.N. Coleman et al., Science 331 (2011) 568–571, https://doi.org/10.1126/science.1194975.
[13] X.J. Huang et al., 2d Materials 3 (2016), https://doi.org/10.1088/2053-1583/3/2/025021. #025021.
[14] X.J. Huang et al., Appl. Phys. Lett. 106 (2015), https://doi.org/10.1063/1.4919935. #203105.
[15] X.J. Huang et al., Sci. Rep. 5 (2015), https://doi.org/10.1038/srep18298. #18298.
[16] J.S. Lee et al., Nanoscale 7 (2015) 3668–3674, https://doi.org/10.1039/c4nr06189f.
[17] K.Y. Shin, J.Y. Hong, J. Jang, Adv. Mater. 23 (2011) 2113, https://doi.org/10.1002/adma.201100345.
[18] L. Edman, B.S.E. McRae, E. Litvin-Staszewska, Phys. Rev. B 57 (1998) 6227.
[19] STMicroelectronics. *M24LR04E-R Datasheet*, <http://www.st.com/resource/en/datasheet/m24lr04e-r.pdf>.
[20] STMicroelectronics. Flex-M24LR04E-R Datasheet, <http://www.st.com/content/ccc/resource/technical/document/data_brief/2d/55/62/05/58/fd/42/e2/DM00058583.pdf/files/DM00058583.pdf/jcr:content/translations/en.DM00058583.pdf>.
[21] NXP_Semiconductors. NXP ICODE SLIX SL2S2002 datasheet, <http://www.nxp.com/documents/data_sheet/SL2S2002_SL2S2102.pdf>.
[22] NXP_Semiconductors. NXP MIFARE Ultralight MF0ICU1 datasheet <http://www.nxp.com/documents/data_sheet/MF0ICU1.pdf>.
[23] O.C. Compton, S.T. Nguyen, Small 6 (2010) 711–723, https://doi.org/10.1002/smll.200901934.
[24] U. Khan et al., Small 6 (2010) 864–871, https://doi.org/10.1002/smll.200902066.
[25] Y.X. Xu et al., J. Am. Chem. Soc. 130 (2008) 5856.
[26] Avanzare. www.avanzare.es.
[27] J.M. Mativetsky et al., J. Am. Chem. Soc. 133 (2011) 14320–14326, https://doi.org/10.1021/ja202371h.
[28] K. Finkenzeller, RFID Handbook: Fundamentals and Applications in Contactless Smart Cards, Radio Frequency Identification and Near-Field Communication, third ed., John Wiley & Sons Inc, 2010.
[29] eDesignSuite v. 8.0.3, 2017.
[30] Computer Aided Three-Dimensional Interactive Application (CATIA).
[31] Standardization, I. O. f. in ISO/IEC 15693-2:2006, 2006.
[32] V. Nicolosi et al., Science 340 (2013) 1420, https://doi.org/10.1126/science.1226419.
[33] Z.Y. Xia et al., Funct. Mater. 23 (2013) 4684–4693, https://doi.org/10.1002/adfm.201370188.
[34] Solvay-Metal-replacement. https://www.technyl.com/en/products-and-solutions/solutions/metal-replacement/index.html.
[35] Y. Lu, Z. Xu, Resour. Conserv. Recycl. 113 (2016) 28–39. doi: 10.1016/j.resconrec.2016.05.007.
[36] D. Ciszewski, T.M. Grygar, Water Air Soil Pollut. 227 (2016) 239, https://doi.org/10.1007/s11270-016-2934-8.
[37] M. Kucki et al., Nanoscale 8 (2016) 8749, https://doi.org/10.1039/c6nr00319b.
[38] J. Russier et al., Nanoscale 5 (2013) 11234–11247, https://doi.org/10.1039/c3nr03543c.
[39] R. Kurapati et al., Small 11 (2015) 3985–3994.
[40] A. Fabbro et al., ACS Nano 10 (2016) 615–623, https://doi.org/10.1021/acsnano.5b05647.
[41] B.M. Blaschke et al., 2d Materials 3 (2016) 8, https://doi.org/10.1088/2053-1583/3/2/025007.
[42] G. Maccaferri et al., Carbon 120 (2017) 165–175, https://doi.org/10.1016/j.carbon.2017.05.030.
[43] M. Akbari et al., Fabrication and characterization of graphene antenna for low-cost and environmentally friendly RFID tags, IEEE Anten. Wirel. Propag. Lett. 15 (2016) 1569–1572, https://doi.org/10.1109/lawp.2015.2498944.
[44] E.B. Secor et al., Gravure printing of graphene for large-area flexible electronics, Adv. Mater. 26 (2014) 4533, https://doi.org/10.1002/adma.201401052.
[45] D.J. Finn et al., Inkjet deposition of liquid-exfoliated graphene and MoS2 nanosheets for printed device applications, J. Materi. Chem. C 2 (2014) 925–932, https://doi.org/10.1039/c3tc31993h.
[46] L. Huang, Y. Huang, J.J. Liang, X.J. Wan, Y.S. Chen, Graphene-based conducting inks for direct inkjet printing of flexible conductive patterns and their applications in electric circuits and chemical sensors, Nano Res. 4 (2011) 675–684, https://doi.org/10.1007/s12274-011-0123-z.